ELSEVIER

Journal of Electroanalytical Chemistry 533 (2002) 119–126

Journal of Electroanalytical Chemistry

www.elsevier.com/locate/jelechem

Voltammetry of a single oil droplet on a large electrode

Porntip Tasakorn, Jingyuan Chen, Koichi Aoki *

Department of Applied Physics, Fukui University, 3-9-1 Bunkyo, Fukui-shi 910-8507, Japan

Received 4 June 2002; received in revised form 5 July 2002; accepted 5 July 2002

Abstract

A nitrobenzene droplet including ferrocene (Fc) was attached to a glassy carbon electrode in aqueous solution so that a three-phase boundary between the water, the oil and the electrode was formed. The question arises as to whether Fc is oxidized at the oil | electrode interface or the oil | electrode | water interface. Hermes and Scholtz proposed the latter interface [Electrochem. Commun. 2 (2000) 845]. We constructed two cells with oil | electrode and oil | electrode | water interfaces, and compared voltammograms for the oil droplet with and without supporting electrolyte. From the dependence of the oxidation current of Fc on potential sweep rate, concentration of Fc, the number of potential scans and the contact area between the oil droplet and the electrode, we found that the peak current in the droplet with supporting electrolyte could be approximated by the conventional voltammetric equation except for the coefficient. In contrast, the effect of the three-phase boundary, i.e. linearity of the current with the radius of the contact area, is conspicuous at high potential scan rates in the droplet without supporting electrolyte.

Keywords: Oil | water interface; Single droplet; Nitrobenzene; Voltammetry of ferrocene; Three-phase boundary

1. Introduction

Most living bodies are composed of a water phase, an oil phase and a fibrous phase. When an electrochemical sensor is inserted into living tissues, the electrode comes in contact with these phases simultaneously. Then the electrode necessarily pierces at least a boundary between two of these phases, and hence a three-phase boundary between the electrode and the two phases is formed. The three-phase boundary can be defined as a line at which three phases meet. Electrode reactions near the three-phase boundary frequently occur when electrochemical sensors are used. However, they have rarely been recognized, probably because of unfamiliar behavior, as well as properties indistinguishable from the usual reactions. The other example of the three-phase boundary is a charge transfer reaction in emulsions [1–7] at which oil droplets including electroactive species are dispersed to a continuous water phase. Some droplets are in contact with the working electrode in a water phase [1,3,7]. The potential of the droplets is controlled with partition of an ion transferring between the oil and the water phase [8–10] and hence redox waves have been observed at potentials different from those for a simple oil | electrode or a water | electrode system [7].

In order to understand the voltammetric behavior of sensors and emulsions clearly, we have to examine the behavior of an electrochemical system simpler than emulsions, for example, a single oil droplet on an electrode immersed in a water phase. Nakatani and coworkers have investigated mass transport of electroactive species at an oil | water interface caused by electrode reactions [11–17]. Their electrochemical system was a single oil droplet (typically ca. 50 μm in diameter) formed so carefully on a microelectrode (10–20 μm in diameter) in the water phase that the electrode was not in contact with the water [18,19]. The product from the electrode reaction transfers from the oil to the water phase in order to maintain the partition equilibrium between the two phases. This mass transfer can be modeled as a series combination of the electrode | oil interface and the oil | water interface. The model is a modification of the cell configuration of the redox species-included oil-coated electrode immersed into water [20,21] from a viewpoint of mass transport.

* Corresponding author. Tel.: +81-776-27-8665; fax: +81-776-27-8494

E-mail address: d930099@icpc00.icpc.fukui-u.ac.jp (K. Aoki).

0022-0728/02/$ - see front matter
PII: S0022-0728(02)01079-3

The other combination of the two interfaces involves the three-phase boundary at which the electrode is exposed to both the oil and the water phase [8,22]. Of interest is an electrode reaction at the three-phase junction when an oil phase contains redox species without deliberately added supporting electrolyte [8,22–28]. The charge transfer reaction requires counterions in order to maintain charge neutrality [23,28]. Since the counterions are present only in the water phase, the reaction should occur at the three-phase boundary, according to the concept of Scholz and coworkers [8,22,28]. Then, the voltammetric current is predicted to be quasi steady-state, like voltammograms at an extremely thin band electrode [29–31]. However, the experimental voltammograms show a conventional waveform [8,22,27]. The other feature of three-boundary phase reactions is the proportionality of the current with the length of the boundary, which is equivalent to the radii of the oil droplets. Although a proportionality has been found [23], the plot involved a large degree of scatter. Marken and coworkers [32,33] carried out a voltammetric study on a three-phase boundary for the redox liquid in aqueous solutions. Although three models and their theoretical voltammograms were presented [34], three-phase boundaries were not identified for the redox liquid system [32,33]. It is, therefore, necessary to re-examine electrode reactions at the three-phase boundary.

In the present paper, voltammetry is carried out at a glassy carbon electrode on which a nitrobenzene (NB) droplet including ferrocene (Fc) is formed in the water phase. The aim is to examine the relationship of the redox current with basic voltammetric variables such as potential sweep rate, concentration, drop size, area of the electrode, the number of potential scans, and the presence or absence of electrolyte in the droplet.

2. Experimental

Two types of electrodes were constructed, as illustrated in Fig. 1. Type (I) is a sessile oil droplet on the electrode surface. The cell is filled with aqueous solution. Since the diameter of the oil droplet is smaller than the diameter of the electrode, a three-phase boundary is formed in a circle on the electrode. This geometry was used by Scholz and coworkers [8,23]. In contrast, type (II) has such a large volume of oil that the oil covers the electrode surface completely. Since the electrode surface is isolated from the water phase by the oil phase, there are two electrode | oil and oil | water interfaces. This geometry is essentially the same as the droplet mounted on the electrode used by Nakatani et al. [12,15,16].

The working electrode was a glassy carbon rod, GC-20S (Tokai Carbon, Tokyo) 6 mm in diameter. After the carbon rod was connected to a conducting wire, its cylindrical side was coated with polytetrafluoroethane tube so that the end of the tube was flush with the electrode surface. The outside of the tube of type (II) was further covered with silicon tube so that the end of the silicon tube was 2 mm above the electrode surface in order to support the oil phase.

The electrochemical cell was a plastic spectroscopic cell ($10 \times 10 \times 40$ mm^3) of which the bottom was drilled and plugged with the electrode. Photographs of the oil droplet were taken through a microscope, Pico Scopeman (Scalar Scopes, Tokyo). Diameters and amounts of oil droplets were evaluated from image analysis with computer software.

The reference electrode was Ag | AgCl in 3 M NaCl solution. The counter electrode was a platinum coil. The potentiostat was a μ-Autolab (Eco Chemie). Nitrobenzene (NB) was purified with 30 vol% of alumina powder for half a day and was separated by filtration. Ferrocene (Fc) (Wako, GR grade) was sublimated and collected in a cooling vacuum flask. Other chemicals were used as received.

The electrode surface was polished with alumina powder and was sonicated in water. After the electrode was inserted into the bottom of the cell, it was sealed with polytetrafluoroethane tape against a leakage of water. The aqueous solution (0.05 M $NaClO_4$) (M: mol dm^{-3}) was poured into the cell for the type (I) electrode, and then a NB droplet was put on the electrode surface using a 5 mm^3 syringe. A screw-driven plunger was installed in the syringe in order to control the volume of injection accurately. When the droplet was mounted on the dry electrode surface after pouring the aqueous solution in the cell, the droplet was sometimes broken into small droplets.

3. Results and discussion

The droplet on the glassy carbon electrode did not move on slanting the electrode, shaking the cell or mixing the solution gently. Fig. 2 shows photographs of Fc-included droplets on the electrode (A) when the droplet did not contain a salt and (B) contained 50 mM tetrabutylammonium perchlorate ($TBAClO_4$). The droplet including the salt was flattened more than the droplet without salt. The former is more hydrophilic than the latter and hence has a larger interfacial energy between the oil and the water. The geometric parameters of the droplet are radii r_1 and r_2 (see the inset of Fig. 3), the former being defined by the radius of the circle on which the droplet meets the electrode, and the latter being the radius of the curvature with which the droplet is regarded as a part of a sphere. We evaluated r_1 and r_2 by use of image analysis, and show the relationship between r_1 and r_2 in Fig. 3. The relation is actually $r_1 =$

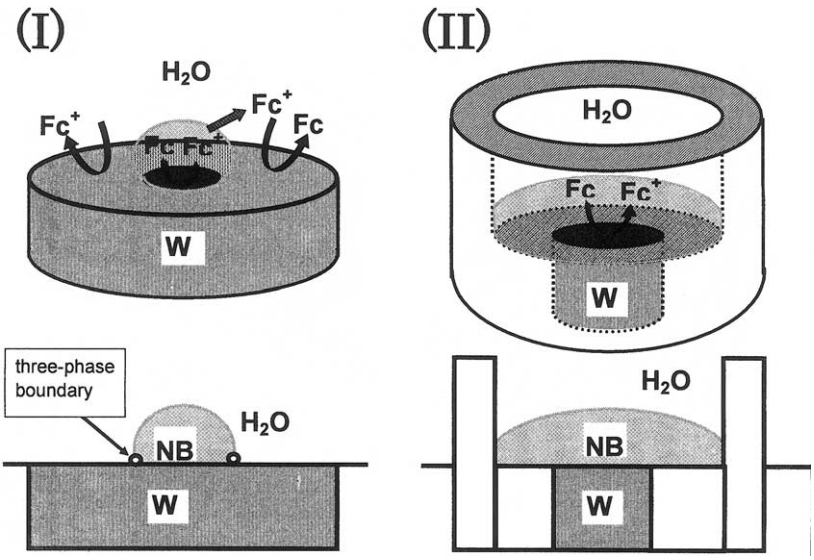

Fig. 1. Illustration of the two types of electrode. Type (I) has an oil droplet smaller than the electrode (W) diameter. It exhibits a three-phase boundary in a circle on the electrode. In type (II), the oil droplet covers the electrode so that the electrode | oil and the oil | water interfaces are formed. Lower illustrations are cross sections of the upper illustrations. Fc is oxidized both in the oil and the water phases in type (I).

r_2, implying that droplets are hemispheres, irrespective of droplet size and inclusion of supporting electrolyte.

Since the oil droplet contains Fc, it may be redox active when it contains supporting electrolyte. The droplet in the cell (I) showed a yellow color when without potential application or at potentials less than 0.4 V. When a potential larger than 0.5 V was applied to the electrode, the yellow turned yellowish green immediately, and then gradually became green. The green faded after a long time of electrolysis. This color change occurred even when the droplet contained no supporting electrolyte. The curvature of the droplet sometimes altered slightly during the potential step application. In contrast, the oil phase in cell (II) showed no color

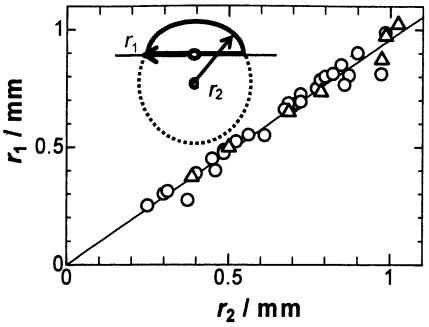

Fig. 3. Variation of r_1 with r_2 for droplets with (triangles) and without (circles) supporting electrolyte. Definitions of r_2 and r_1 are depicted in the inset.

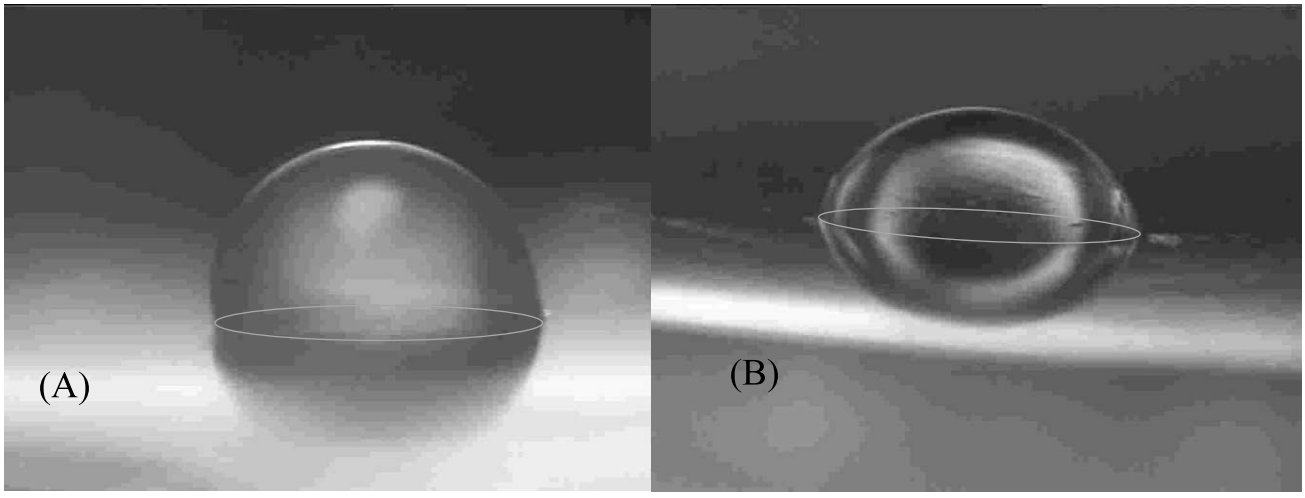

Fig. 2. Photographs of a NB droplet on the glassy carbon electrode in an aqueous solution of 50 mM $NaClO_4$. The droplet contained (A) 1 mM Fc and (B) 1 mM Fc+50 mM $TBAClO_4$. Radii of the droplets are 0.5 mm.

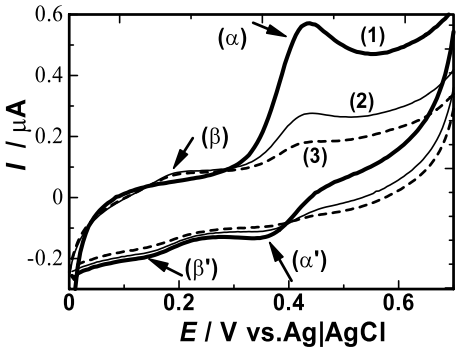

Fig. 4. Cyclic voltammograms of the oil droplet in a type (I) cell at a potential sweep rate of 10 mV s^{-1}. The oil phase contained 50 mM $TBAClO_4$ whereas the water phase contained 50 mM $NaClO_4$. Geometry of the droplet was $r_1 = 0.50$ mm and $r_2 = 0.56$ mm. Numbers (1), (2) and (3) denote the first, the second and the third scan.

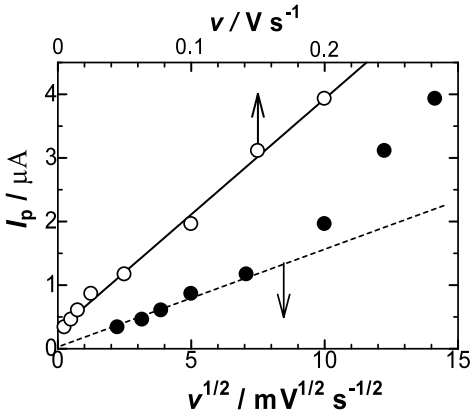

Fig. 5. Dependence of the peak current of the wave (α) in the first potential scan in the type (I) cell on the square-root of scan rates when the oil droplet contained 50 mM $TBAClO_4$. Size of the droplet is $r_1 =$ 0.6 mm.

change after a potential application for a few minutes, because it is too thick (2 mm) to allow oxidation of Fc within the oil phase.

Fig. 4 shows cyclic voltammograms of the droplet in which 0.05 M $TBAClO_4$ was included in cell (I). The voltammogram of the first scan shows a large anodic peak at 0.44 V (α), a cathodic peak at 0.34 V (α′) and a small cathodic peak at 0.16 V (β′). Waves (α) and (α′) are obviously a redox pair of Fc in the oil phase. The voltammogram in the second scan has not only waves (α), (α′) and (β′) but also a small anodic wave at 0.20 V (β). Waves (α) and (α′) decreased with an increase in the iterative potential scan, implying depletion of Fc in the droplet. It is predicted that Fc in the oil is oxidized (wave (α)) at the electrode to yield ferrocenium ion (Fc^+), which is dissolved in the water phase. Then, the local concentration of Fc^+ in the oil decreases and hence the reduction wave of Fc^+ also decreases after multiple scans. The Fc^+ transferred to the water phase gives the reduction wave (β′) for which the potential is the same as the reported value [35]. The reduced Fc is oxidized in the water phase to give wave (β). This wave did not appear in the first scan but did in the second and succeeding scans. This observation supports the suggestion that Fc in the water phase can be ascribed to the potential sweep over 0.5 V. The reaction mechanism is illustrated in Fig. 1(I).

Values of the peak current, I_p, for wave (α) at the first scan were plotted against the potential sweep rate, v, and its square-root in Fig. 5. The current value at a given v was the average of three currents at newly formed droplets. The dependence of I_p on v is linear but not proportional, whereas the dependence of I_p on $v^{1/2}$ has no linear relation. The variation of $\log(I_p)$ with $\log(v)$ has a linear relation with a slope of 0.66. Therefore, the peak current is under mixed control by finite diffusion and infinite diffusion. In order to demonstrate the mixed control, we compare the diffusion thickness with the drop size. The elapsed time from the current rise to the peak (α) in Fig. 4 is approximately 10 s. Then the thickness of the diffusion layer is 0.1 mm for a diffusion coefficient of 10^{-5} cm^2 s^{-1}. This value is much smaller than the radius of the droplet (0.6 mm), and I_p should behave as at infinite diffusion. However, the diffusion domain near the oil | water | electrode boundary is very small owing to the geometrical limitations, and hence the diffusion layer near the oil | water | electrode boundary soon reaches the hemispherical surface of the oil droplet. Consequently the current is controlled by both infinite and finite diffusion.

The question arises as to whether Fc in the oil droplet is dissolved in the water phase, which decreases the concentration of Fc or I_p even in the reduced state. In order to examine the possibility of a dissolution, we left a newly formed droplet for a given time, at most 30 min, in the reduced state and obtained I_p by linear sweep voltammetry. The dependence of I_p on the time, t, that the droplet was left in the aqueous solution is shown in Table 1. The peak current is independent of the time, indicating a negligible amount of dissolution of Fc in the aqueous solution without electrochemical oxidation. Therefore, it is not necessary to take into account the dissolution of Fc in the reduced state.

Cyclic voltammograms for cell (II) are shown in Fig. 6. The anodic and cathodic waves correspond to waves

Table 1
Variation of the α peak current in Fig. 4 with the time of leaving the oil droplet in the aqueous solution

t/min	I_p/μA
0	1.33 ± 0.08
1	1.20 ± 0.18
15	1.30 ± 0.16
30	1.35 ± 0.04

Potential scan started t min after the droplet was formed on the electrode in the aqueous solution.

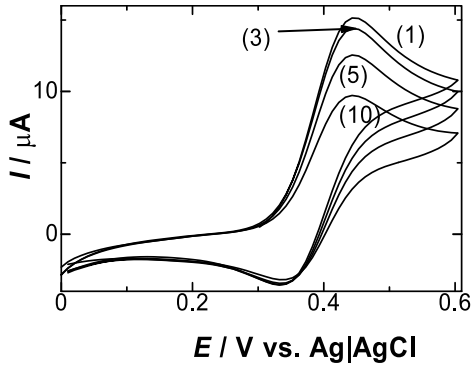

Fig. 6. Cyclic voltammograms of the oil droplet in the type (II) cell at a potential sweep rate of 10 mV s^{-1}. The number (n) denotes the voltammogram observed in the n-th scan. The oil phase contained 50 mM $TBAClO_4$ whereas the water phase contained 50 mM $NaClO_4$.

(α) and (α′) in cell (I) of Fig. 4. Although the iterative potential scan decreased the peak currents, the decrease is much smaller than that in cell (I) (see Fig. 4). The decrease is obviously due to the dissolution of Fc^+ in the water phase. Values of I_p for the anodic wave in the first scan were proportional to $v^{1/2}$ in the range from $2 < v^{1/2} < 15$ $mV^{1/2}$ $s^{-1/2}$. These facts imply that the electrode reaction can be regarded as the usual behavior of Fc in NB at a large electrode if the scan number is less than 3.

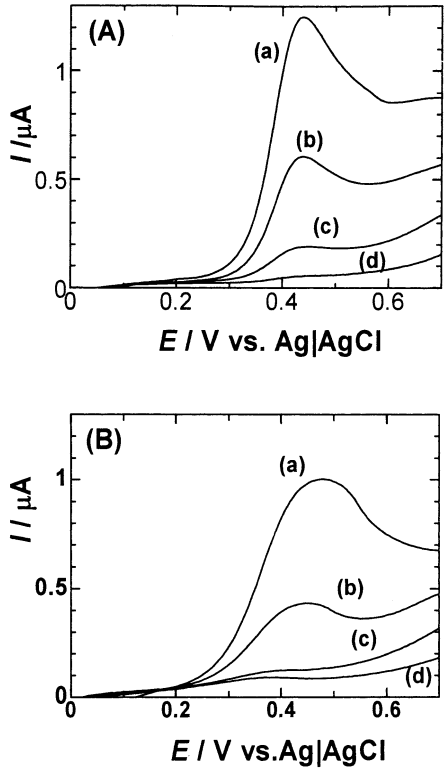

Fig. 7. Linear sweep voltammograms of the oil droplet for $0.50 < r_1 < 0.62$ mm at $v = 10$ mV s^{-1} when the oil contained (A) c mM Fc + 50 mM $TBAClO_4$ and (B) c mM Fc, where c is (a) 2.5, (b) 1.0, (c) 0.1 and (d) 0.05 mM. The water phase contained 50 mM $NaClO_4$.

Linear sweep voltammograms for cell (I) are shown for several concentrations of Fc in Fig. 7(A). The peak potential did not vary with the concentration of Fc, suggesting no IR-drop effect. The mixed control discussed in Fig. 5 can also be demonstrated by comparison between the oxidation charge and the latent redox charge in the droplet, as follows: the oxidation charge in curve (a) of Fig. 7(A) is approximately 15 μC if the background current is assumed to be at 0.6 V, whereas the total charge of Fc in the droplet is 50 μC. Obviously the former is not so negligible as the latter. The oxidation in the oil phase is necessarily accompanied with transfer of perchlorate ion from the water to the oil in order to satisfy electrical neutrality. The absence of supporting electrolyte in the oil phase might prevent the oxidation of Fc. Thus, we attempted to perform voltammetry without supporting electrolyte, and show the voltammograms in Fig. 7(B). Although wave (α) shifted slightly in the more positive direction with an increase in the concentration, well-defined peaks can be recognized. This is because diffusion of perchlorate ion from the water to the oil is faster than the potential sweep rate.

When the cell (II) was employed without supporting electrolyte, waves similar to Fig. 7(B) are expected to be observed at low potential sweep rates. Nevertheless, no peak was observed even at a very slow sweep rate ($v =$ 0.5 mV s^{-1}), as is shown in Fig. 8. The maximum current value at the first scan was only 1% of the peak current that was obtained under the same conditions, except for the addition of 50 mM $TBAClO_4$. The current increased with the time of the voltammetry, suggesting gradual insertion of an ionic impurity into the oil phase.

Peak currents in Fig. 7 seem to show a linear variation with the concentration of Fc. In order to examine the variation in detail, we plotted I_p of the wave (α) at the first scan against concentration of Fc, c, in Fig. 9 on logarithmic scales. Plots for droplets with and without electrolyte except for $c = 0.05$ mM fell on straight lines

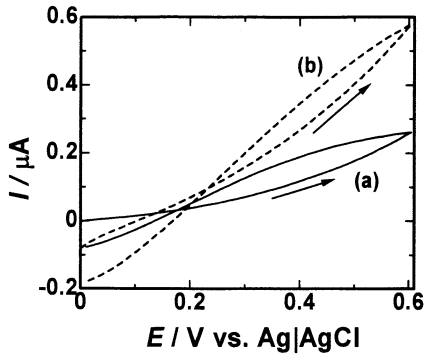

Fig. 8. Voltammograms of the oil droplet containing 1 mM Fc without supporting electrolyte in cell (II) at $v = 0.5$ mV s^{-1} for the first (a) and the second (b) scan. The water phase contained 50 mM $NaClO_4$.

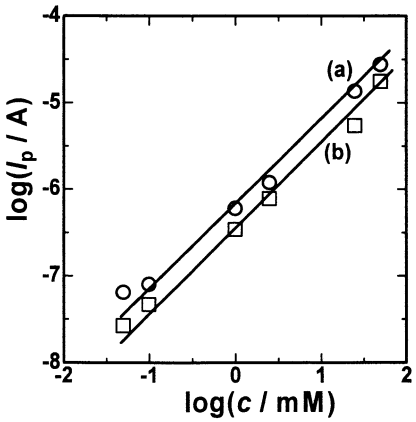

Fig. 9. Logarithmic variation of I_p with c (concentration of Fc) in cell (I) at $v = 10$ mV s^{-1}. The droplet ($r_1 = 0.52$ mm) contained (a) c mM Fc+50 mM $TBAClO_4$ and (b) c mM Fc.

with unit slope. The upper deviation at $c = 0.05$ mM may be due to insufficient subtraction of the residual current. The slope without supporting electrolyte was 60% of that with the supporting electrolyte. This decrease in the current is ascribed partly to the roundness of the peak shape owing to the IR-drop, as is seen in Fig. 7(B) and partly to a delay of diffusion of perchlorate ion to the reaction site from the water phase.

Values of I_p of the wave (α) for the droplet including 50 mM $TBAClO_4$ were plotted against the contact area, πr_1^2, of the oil droplet with the electrode in Fig. 10. Good proportionality is found for any concentration of Fc. From the proportionality of I_p with the concentration (Fig. 9), with $v^{1/2}$ (Fig. 5) and with πr_1^2 (Fig. 10), the oxidation of Fc in the cell (I) behaves as if it might occur at the hypothetical electrode, radius r_1, as illustrated in Fig. 11. In this model, Fc is present uniformly in NB before the oxidation. In other words, the water phase plays a part in the supply of perchlorate ion as well as an acceptor of Fc^+. This model infers the validity of the equation for the diffusion-controlled peak current of the

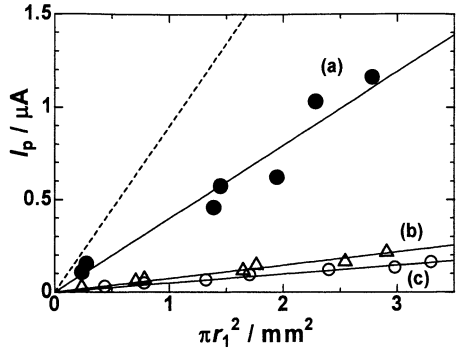

Fig. 10. Variations of I_p in the first scan in cell (I) with the contact area of the oil | electrode interface, πr_1^2 when the droplet contained c mM Fc+50 mM $TBAClO_4$, where c is (a) 1.0, (b) 0.1 and (c) 0.05 mM. The scan rate was 10 mV s^{-1}. The dashed line was calculated from Eq. (1) for $c = 1$ mM, $D = 10^{-5}$ cm^2 s^{-1} and $v = 10$ mV s^{-1}.

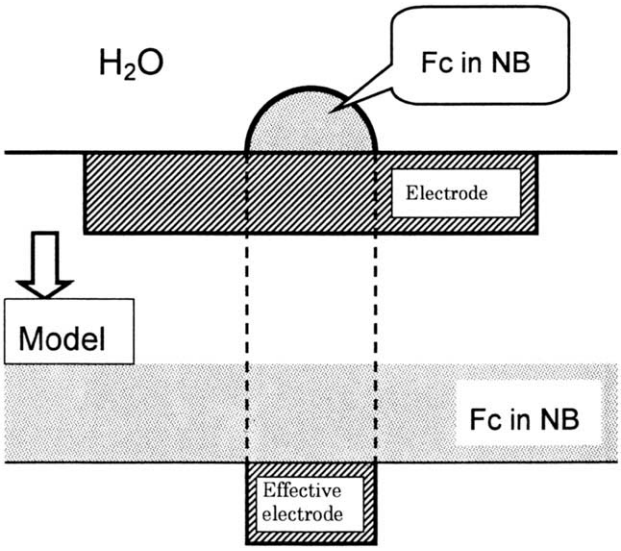

Fig. 11. A mass-transfer model (lower) for the oxidation of Fc in the oil droplet (upper).

reversible reaction, given by

$$I_p = 0.4463(F^3/RT)^{1/2}(\pi r_1^2)c(Dv)^{1/2} \quad (1)$$

where D is the diffusion coefficient of Fc in the oil phase. By use of $D = 10^{-5}$ cm^2 s^{-1}, the value calculated from Eq. (1) is 160% larger than the experimental value, as is shown in the dashed line in Fig. 10.

The oxidation in the droplet without supporting electrolyte should occur at the three-phase boundary [23], i.e. on the circumference of the circle, radius r_1, partly because the oil phase is very resistive and partly because the oxidation requires charge compensation by anions in order to satisfy electrical neutrality. From this prediction, the peak currents observed without supporting electrolyte at $v = 10$ mV s^{-1} were plotted against r_1 (not shown here). Unfortunately, no proportionality was found. We re-plotted them against the contact area of the droplet (πr_1^2) in Fig. 12. Good proportionality was found in the domains $0.05 < c < 50$ mM and $0.1 < r_1 < 0.55$ mm. Under these conditions, the peak current can be regarded as due to reactions at the oil | electrode interface rather than those at the three-phase boundary.

It is predicted that the effect of the three-phase boundary, i.e. the proportionality of I_p with r_1, may be distinct at such a short time [28] that the anion (perchlorate ion) for the charge compensation of Fc^+ diffuses only to the edge of the droplet but does not reach the whole oil | electrode interface. Rapid scan rates at large droplets may make the effect of the three-boundary distinct. Fig. 13 shows variation of I_p with r_1 for fast and slow potential sweep rates. The faster the sweep rate, the better is the proportionality found. Re-plotting I_p against r_1^2 (the upper x-axis) in Fig. 13 demonstrates the deviation from the line for the I_p

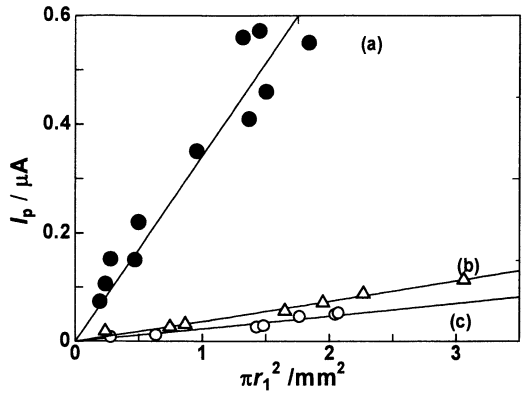

Fig. 12. Variations of I_p at the first scan in the cell (I) with the contact area of the oil | electrode interface, πr_1^2 when the droplet contained c mM Fc without supporting electrolyte, where c is (a) 1.0, (b) 0.1 and (c) 0.05 mM. The scan rate was 10 mV s^{-1}.

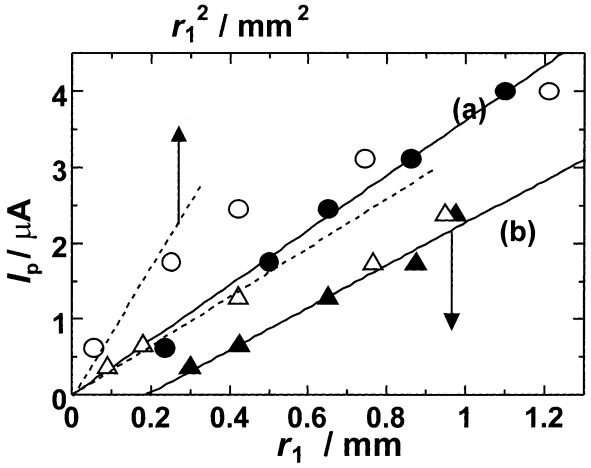

Fig. 13. Dependence of I_p in the first scan in cell (I) on the radius, r_1, (on the lower axis, filled symbols) and contact area, πr_1^2 (on the upper axis, open symbols) of the droplet at $c = 5$ mM without supporting electrolyte. Potential sweep rates are (a) 50 and (b) 5 mV s^{-1}. The dashed lines were drawn to show the proportionality fitted for $I_p < 1.8$ μA.

versus r_1^2 plot at 50 mV s^{-1}. In contrast, the proportionality of I_p versus r_1^2 is valid at 5 mV s^{-1}.

On the basis of the above experimental results, we propose the following model for the effect of the three-phase boundary. The oxidation of Fc requires a counterion, which is supplied from the water phase by diffusion into the oil phase. In a short time electrolysis, the counterion inserted into the oil phase is localized around the three-phase boundary. As the time lapses, the diffusion layer of the counterion is expanded toward the center of the circular oil | electrode interface. The oxidation occurs at the part of the electrode, which the diffusion layer can reach. In other words, it occurs preferentially on the ring of the oil | electrode interface at short times, as is shown in Fig. 14. We let its diffusion thickness be δ. Then the diffusional behavior at the ring

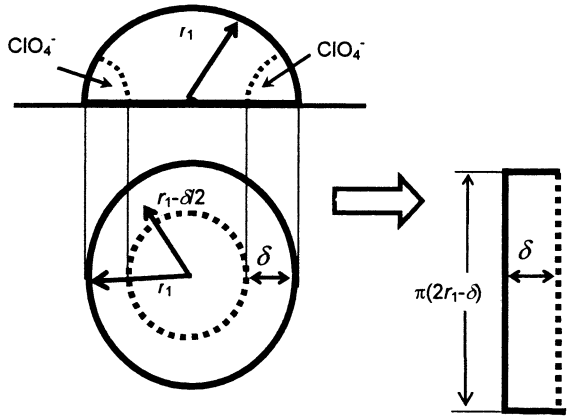

Fig. 14. A model of the three-phase boundary. Diffusion of ClO_4^- reaches the ring domain δ wide, at which Fc is oxidized. The left hand side shows the band electrode modeled after the ring.

can be regarded as that at the band $\pi(2r_1-\delta)$ long and δ wide (the left hand side in Fig. 14) if $\delta \ll r_1$. Then the current may be approximated from the mass-transfer equation for the band electrode. The equation for the chronoamperometric current at a band electrode has been given by [30]

$$I = FcD\pi(2r_1 - \delta)((\pi Dt)^{-1/2}\delta + 0.97 - 1.10\exp[-9.90/|\ln(12.37Dt/\delta^2)|]) \quad (2)$$

where we replaced the length and the width of the band electrode by $\pi(2r_1-\delta)$ and δ, respectively. Eq. (2) for a short time electrolysis becomes $\pi^{1/2}Fc(2r_1-\delta)\delta(D/t)^{1/2}$, which is almost proportional to r_1. This agrees with the variation at $v = 50$ mV s^{-1} in Fig. 13. In contrast, a long electrolysis increases δ to r_1, and finally the diffusion layer covers the whole oil | electrode interface. Then the oxidation occurs at the whole interface, and the current is proportional to the interfacial area, πr_1^2.

As a confirmation of the above model, we estimated δ approximately. The sweep rates, 5 and 50 mV s^{-1}, are equivalent to electrolysis times of 40 and 4 s, respectively, when the peak appears after 200 mV from the beginning of the effective electrolysis (see Fig. 7(B)). The corresponding diffusion distances are $\delta = (Dt)^{1/2} = (10^{-5}$ cm s^{-1} $\times$ (40 and 4 s))$^{1/2} = 0.20$ and 0.063 mm, respectively. Typical values of r_1 in the present experiment range from 0.2 to 0.4 mm. Therefore, the condition of $v = 5$ mV s^{-1} makes the diffusion layer cover the whole oil | electrode interface, whereas that of $v = 50$ mV s^{-1} makes it localized near the edge of the interface.

4. Conclusion

When the oil droplet in cell (I) contains supporting electrolyte, the oxidation current of Fc in the oil droplet is controlled by diffusion of Fc, i.e. it is proportional to the concentration, the square root of the potential sweep

rate for $v < 0.1\ \mathrm{V\ s^{-1}}$ and the contact area of the droplet on the electrode. The peak current can be expressed in terms of the conventional expression for the reversible peak current, except for the coefficient, if the electroactive area is taken to be the area of the oil | electrode interface. Experimental values are about half the values calculated from the conventional equation because of the finite diffusion effect.

The effect of the three-phase boundary, i.e. the proportionality of the peak current with the radius of the circular oil | electrode interface, becomes conspicuous when the scan rate becomes faster without supporting electrolyte. Diffusion of the counterion at a short time restricts the electrode reaction to the edge of the oil | electrode interface. This behavior can be modeled as a diffusion current at a microband electrode. With the lapse of time, the diffusion layer extends toward the center of the circular interface, and finally covers the interface. Then the oxidation occurs over the whole interface area, not at the three-phase boundary. Consequently, the effect of the three-phase boundary diminishes with time and finally cannot be detected. In other words, electrode reactions at a genuine three-phase boundary rarely occur.

Acknowledgements

This work was financially supported by Grants-in-Aid for Scientific Research (Grants 14340232 and 14540556) from the Ministry of Education in Japan.

References

[1] T. Matsubara, J. Texter, J. Colloid Interf. Sci. 112 (1986) 421.
[2] J. Texter, T. Beverly, S.R. Templar, T. Matsubara, J. Colloid Interf. Sci. 120 (1987) 389.
[3] J. Georges, S. Desmettre, Electrochim. Acta 31 (1986) 1519.
[4] J. Georges, J.W. Chen, Colloid Polym. Sci. 264 (1986) 896.
[5] F. Marken, R.G. Compton, Electrochim. Acta 43 (1998) 2157.
[6] T. Kakiuchi, Electrochem. Commun. 2 (2000) 317.
[7] J. Chen, O. Ikeda, K. Aoki, J. Electroanal. Chem. 496 (2001) 88.
[8] F. Scholz, S. Komorsky-Lovric, M. Lovric, Electrochem. Commun. 2 (2000) 112.
[9] H.H.J. Girault, D.J. Schiffrin, in: A.J. Bard (Ed.), Electroanalytical Chemistry, A Series of Advances, vol. 15, Marcel Dekker, New York, 1989, p. 1.
[10] J. Koryta, P. Vanysek, in: H. Gerischer, C.W. Tobias (Eds.), Advances in Electrochemistry and Electrochemical Engineering, vol. 12, Wiley, New York, 1981, p. 113.
[11] K. Nakatani, K. Chikama, N. Kitamura, in: D.C. Neckers, D.H. Volman, G. von Bunau (Eds.), Advances in Photochemistry, Wiley, New York, 1999.
[12] K. Nakatani, T. Uchida, H. Misawa, N. Kitamura, H. Masuhara, J. Phys. Chem. 97 (1993) 5197.
[13] K. Nakatani, T. Uchida, N. Kitamura, H. Masuhara, J. Electroanal. Chem. 375 (1994) 383.
[14] K. Nakatani, T. Uchida, H. Misawa, N. Kitamura, H. Masuhara, J. Electroanal. Chem. 367 (1994) 109.
[15] K. Nakatani, M. Wakabayashi, K. Chikama, N. Kitamura, J. Phys. Chem. 100 (1996) 6749.
[16] K. Nakatani, M. Suda, N. Kitamura, J. Phys. Chem. B 102 (1998) 2908.
[17] N. Terui, K. Nakatani, N. Kitamura, J. Electroanal. Chem. 494 (2000) 41.
[18] K. Nakatani, T. Sekine, J. Colloid Interf. Sci. 225 (2000) 251.
[19] K. Nakatani, T. Sekine, Langmuir 16 (2000) 9256.
[20] C. Shi, F.C. Anson, J. Phys. Chem. B 102 (1998) 9850.
[21] C. Shi, F.C. Anson, J. Phys. Chem. B 103 (1999) 6283.
[22] S. Komorsky-Lovric, M. Lovric, F. Scholz, J. Electroanal. Chem. 508 (2001) 129.
[23] M. Hermes, F. Scholz, Electrochem. Commun. 2 (2000) 845.
[24] C.-L. Chang, T.-C. Lee, T.-J. Huang, J. Solid State Electrochem. 2 (1998) 291.
[25] K.B. Oldham, J. Solid State Electrochem. 2 (1998) 367.
[26] H. Fukunaga, M. Ihara, K. Sakaki, K. Yamada, Solid State Ionics 86/88 (1996) 1179.
[27] R. Gulaboski, V. Mirceski, F. Scholz, Electrochem. Commun. 4 (2002) 277.
[28] M. Donten, Z. Stojek, F. Scholz, Electrochem. Commun. 4 (2002) 324.
[29] K. Aoki, K. Tokuda, H. Matsuda, J. Electroanal. Chem. 225 (1987) 19.
[30] K. Aoki, K. Tokuda, H. Matsuda, J. Electroanal. Chem. 230 (1987) 61.
[31] K. Aoki, K. Tokuda, J. Electroanal. Chem. 237 (1987) 163.
[32] J.C. Ball, F. Marken, Q. Fulian, J.D. Wadhawan, A.N. Blythe, U. Schroeder, R.G. Compton, S.D. Bull, S.G. Davies, Electroanalysis 12 (2000) 1017.
[33] F. Marken, C.M. Hayma, P.C. Bulma Page, Electrochem. Commun. 4 (2002) 462.
[34] Q. Fulian, J.C. Ball, F. Marken, R.G. Compton, A.C. Fisher, Electroanalysis 12 (2000) 1012.
[35] Y. Ohsawa, S. Aoyagui, J. Electroanal. Chem. 136 (1982) 353.